Agricultural and Forest Meteorology 191 (2014) 1–11

Contents lists available at ScienceDirect

Agricultural and Forest Meteorology

journal homepage: www.elsevier.com/locate/agrformet

Monitoring the effects of rapid onset of drought on non-irrigated maize with agronomic data and climate-based drought indices

Eric D. Hunt[a,f,*], Mark Svoboda[b], Brian Wardlow[c], Kenneth Hubbard[d], Michael Hayes[b], Tim Arkebauer[e]

[a] School of Natural Resources, University of Nebraska–Lincoln, Lincoln, NE, United States
[b] National Drought Mitigation Center, School of Natural Resources, University of Nebraska–Lincoln, Lincoln, NE, United States
[c] Center for Advanced Land Management Information Technologies, School of Natural Resources, University of Nebraska–Lincoln, Lincoln, NE, United States
[d] High Plains Regional Climate Center, School of Natural Resources, University of Nebraska–Lincoln, Lincoln, NE, United States
[e] Department of Agronomy and Horticulture, University of Nebraska–Lincoln, Lincoln, NE, United States
[f] Atmospheric and Environmental Research, Inc., Lexington, MA, United States

ARTICLE INFO

Article history:
Received 14 January 2013
Received in revised form
31 December 2013
Accepted 2 February 2014
Available online 28 February 2014

Keywords:
Soil water
Flash drought
Stomatal conductance
Drought index
Evapotranspiration
Gross primary productivity

ABSTRACT

The 2003 growing season at Mead, NE began with moist and relatively cool conditions that persisted through most of June. During this moist phase of the season, soil water and parameters such as evapotranspiration (ET) and gross primary productivity (GPP) were nearly identical between a rainfed maize site (RMS) and an irrigated maize site (IMS). A drying phase began in late June, causing decline in soil water at RMS and the necessity of irrigation treatments at IMS. The drying phase turned into a "stressed" phase by early August, as only 10 mm of precipitation fell in a 40-day period between mid-July and late August. Conditions at RMS began to deteriorate even more rapidly after maize entered the critical reproductive stage, as the depletion of soil water led to (implied) reductions in stomatal conductance, which led to significant reductions in ET and GPP, compared to the well-watered IMS. Two drought indices, the Standardized Precipitation Index (SPI) and the Standardized Precipitation Evapotranspiration Index (SPEI), were utilized to show the effectiveness of short-term indices at detecting flash drought versus field measurements. Results showed that both the 1-month SPI and the 1-month SPEI were quite sensitive to the onset of the flash drought and closely followed the decline in soil water and other biophysical parameters at RMS relative to IMS. Significant precipitation returned and led to some recharge prior to harvest but was far too late to be of any help to the maize at RMS, as the yield difference of 6.3 Mg/ha between RMS and IMS revealed the detrimental effects of a rapid onset of drought during the critical reproductive stage of maize.

1. Introduction

Soil water is an integral part of the hydrologic cycle and a critical parameter for plant growth and development. Dale and Shaw (1965) reported that soil water is one of the most critical factors for crop development and yield. Soil water stress at the silking stage of maize (*Zea mays* L.) can reduce grain yield by 50% (Denmead and Shaw, 1960) and an omission of a single irrigation treatment at a critical stage could reduce maize yields by up to 40% (Cakir, 2004). Meyer et al. (1993) reported that maize was most sensitive to water stress in the silking-blister dough stage and Calvino et al. (2003) showed a curvilinear response of maize yield to available water in the three weeks preceding and following silking. Earl and Davis (2003) reported maize yield reductions up to 85% during severe water stress that occurred after the sixth leaf stage in Georgia. Thus, it is well established that a lack of soil water causes stress and yield reduction in maize. But soil water is not a commonly measured variable at NOAA Cooperative (COOP) weather stations and there are but a handful of networks around the United States where soil water is a standard, quality controlled observation (Hollinger and Isard, 1994; Illston et al., 2008; Hubbard et al., 2009).

Drought is a natural, recurring phenomena that occurs everywhere at various points in time and is occurring somewhere on Earth at any given point of time. Drought is a complex topic with ecosystem impacts that vary with its intensity and duration and socio-economic impacts that often magnify problems for the most vulnerable members of society. Perhaps it is fitting that drought does not have a universal definition and is often considered in the context of four broad categories defined by Wilhite and Glantz

* Corresponding author at: Atmospheric and Environmental Research, Lincoln, NE, United States. Tel.: +1 402 294 3616.
E-mail address: ehunt@aer.com (E.D. Hunt).

0168-1923/$ – see front matter © 2014 Elsevier B.V. All rights reserved.
http://dx.doi.org/10.1016/j.agrformet.2014.02.001

(1985): meteorological, agricultural, hydrological, and socioeconomic.

Short-term drought, sometimes referred to as flash drought, is a rapid onset of drought often accompanied by high temperatures and winds that lead to rapid soil moisture depletion during a critical time in the growing season (Svoboda et al., 2002). Flash droughts can occur within a longer period of normal or above normal precipitation and bring devastating agricultural impacts. For example, although precipitation was above normal in most of Oklahoma during 1998, an intense, short-term drought during the summer decimated the state's cotton and peanut crop (Basara et al., 1998; Illston and Basara, 2003). Illston et al. (2004) described four phases of soil moisture in a flash drought case in Oklahoma: a moist plateau in the spring, transitional drying early in the summer, enhanced drying mid-summer into early autumn, and recharge during the cooler months of late autumn and winter.

The 2003 growing season at Mead, NE closely matches the description of flash drought given in Svoboda et al. (2002). It began with moist and cool conditions that persisted through much of June. However, a prolonged period of minimal precipitation with periodic spells of heat led to a rapid decline in soil water at a rainfed maize site compared to a nearby irrigated site, which led to significant reductions in biophysical parameters such as evapotranspiration (ET) and gross primary productivity (GPP). The time series of soil moisture from the growing season at the rainfed maize site closely follows the four phases introduced in Illston et al. (2004). Thus, the primary goal of this paper is to show the relationship between soil water and agroecological parameters (ET and GPP) during four phases of the growing season. A secondary goal of this paper is to show the utility of using short-term and longer-term drought indices for monitoring a flash drought that occurred during the critical reproductive stage of maize at a rainfed site. The remainder of this section describes a short history of drought indices, with a particular focus on the two normalized drought indices used in this study – the Standardized Precipitation Index (SPI) and the Standardized Precipitation Evapotranspiration Index (SPEI).

Palmer (1965) developed the Palmer Drought Severity Index (PDSI) with an objective of "developing a general methodology for evaluating drought in terms of an index that permits time and space comparisons of drought severity." The PDSI is calculated from a simple water balance model that uses factors such as precipitation, temperature and latitude for the calculation of potential evapotranspiration (Thornthwaite, 1948), recharge, runoff, and soil moisture loss to determine whether recent precipitation was sufficient to maintain a normal water balance. The PDSI is divided into 11 categories ranging from extreme drought to extreme wet spell (Heim, 2002).

McKee et al. (1993) developed the Standardized Precipitation Index (SPI) in response to demand from Colorado decision makers for an index that expressed current conditions in terms of water supply, deficit, and probability. The SPI has the advantage of being spatially invariant and an indicator of drought on multiple time scales (Guttman, 1999), though caution has been advised when comparing the SPI between sites with very different periods of record and at short time scales during distinct dry seasons (Wu et al., 2005).

The SPI has been widely used for operational and research purposes. Hayes et al. (1999) showed that the SPI detected drought conditions a full month ahead of the PDSI during the U.S. southern Plains drought of 1996. Livida and Assemakopoulos (2007) used the SPI to show that mild and moderate drought were more common on the 3- and 6-month time scale across northern Greece while severe drought was more frequent across southern Greece. Brown et al. (2008) integrated the SPI with satellite derived vegetation metrics and biophysical data to produce 1-km maps of the Vegetation Drought Response Index (VegDRI). McRoberts and Nielsen-Gammon (2012) used daily precipitation from the Advanced Hydrologic Prediction Service multisensor precipitation estimates (MPE) and COOP station data to obtain a high resolution SPI to be used as guidance for the U.S. Drought Monitor (Svoboda et al., 2002). Thus, it was recommended by the World Meteorological Organization to be the primary drought index for national meteorological and hydrological agencies in monitoring meteorological drought across the globe (Hayes et al., 2011).

One criticism of a precipitation-only index like the SPI is that it does not account for temperature effects on drought. For example, Hu and Willson (2000) showed that the temperature and precipitation dependent PDSI was affected by both large anomalies of temperature and precipitation in the central United States. Vicente-Serrano et al. (2010) addressed this issue with the development of the SPEI. The SPEI is based on the monthly (or weekly) difference between precipitation and potential evapotranspiration (ET_p), using the ET_p method from Thornthwaite (1948). The Thornthwaite method of ET_p was chosen over more robust methods, such as the Penman–Monteith (Monteith, 1964), due to the simplicity of its calculation and its reasonable performance when calculating a drought index, such as the PDSI (Mavromatis, 2007).

The development of drought indices allows for useful comparisons of conditions between locations and over long periods of time. However, caution should still be applied when applying an index to long time-series of climate data. Inhomogeneities in data from station relocations, instrumentation changes, and growth of vegetation and urban boundaries do exist and analyses can be erroneous if these items are not accounted for (Peterson et al., 1998). Nevertheless, climate-based drought indices are useful at identifying the severity and duration of drought and continued research will only make existing indices more accurate and robust.

2. Materials and methods

2.1. Study site

The CSP is located at the University of Nebraska-Lincoln (UNL) Agricultural Research and Development Center near the town of Mead, NE. The CSP commenced in the spring of 2001 and consists of three sites. The first agroecosystem is an irrigated, continuous maize (ICM) site centered at 41°09′54.2″ N, 96°28′35.9″ W with an irrigated area of 48.7 ha. The second agroecosystem is an irrigated, rotated maize-soybean (IMS) site centered at 41°09′53.5″ N, 96°28′12.3″ W with an irrigated area of 52.4 ha. Both ICM and IMS were irrigated rotations of maize and soybeans under no-till in the 10 years prior to the initialization of the CSP. The third agroecosystem is a rain-fed, rotated maize-soybean (RMS) site centered at 41°10′46.8″ N, 96° 26′22.7″ W with an area of 65.4 ha. Prior to the CSP, RMS had 2–4 ha plots of maize, soybeans, wheat, and oats with tillage (Verma et al., 2005). ICM was not considered in this analysis as its management practice (i.e., continuous maize) made it less comparable to RMS than IMS.

Each CSP site consists of six, 20 m × 20 m intensive management zones, hereafter referred to as IMZ's, where detailed process-level studies of soil water, soil carbon dynamics, canopy and soil gas exchange, crop growth and biomass partitioning are established. Prior to the onset of the CSP in 2001, all three sites were uniformly tilled by disking the top 10 cm to incorporate Phosphorous (P) and Potassium (K) fertilizers and to homogenize the soil layer (Suyker and Verma, 2009). Nitrogen (N) fertilizer applications were applied to IMS and RMS prior to planting in 2003; subsequent N applications were applied in June at IMS through the center-pivot system in a process known as fertigation.

The IMZ locations were selected using *k*-means clustering applied to six layers of 4 m × 4 m cells based broadly on soil type,

topography, and crop production potential within each site. Fine-scale spatial information used for each site included a digital soil map, a digital elevation model, a Veris map of soil electrical conductivity (0–30 cm), near infrared reflectance of bare soil from the IKONOS satellite (4 km resolution), and a map of soil organic matter (0–20 cm). Interpolation onto a 4 m × 4 m grid was done by kriging.

2.2. Eddy covariance flux method and measurement

Toward the middle of each field is an eddy covariance tower installed for measurements of CO_2 and H_2O fluxes. The eddy covariance method is used to measure the exchange of CO_2 and H_2O between the biosphere and atmosphere at over a hundred sites worldwide and has produced defensible estimates of carbon exchange. The method works by sampling atmospheric turbulence to determine the net difference of material going across the atmosphere-canopy interface (Baldocchi et al., 1988; Baldocchi, 2003).

CO_2 fluxes were measured with an array of sensors – a three-dimensional sonic anemometer (R3, Gill Instruments Ltd., Lymington, UK) and a closed-path CO_2/H_2O system (LI 6262, Li-Cor Inc., Lincoln, NE). H_2O fluxes were measured with an open-path CO_2/H_2O sensor (LI 7500, Li-Cor Inc., Lincoln, NE). Further details are given in Verma et al. (2005) and Suyker et al. (2003). Eddy covariance sensors were mounted at a height of 3.0 m above the ground until canopy height exceeded 1.0 m. When canopy height exceeded 1.0 m, the eddy covariance sensors were moved to a height of 6.0 m, a height they remained at until harvest.

The CO_2 storage in the layer below the eddy covariance sensors was calculated from CO_2 concentration profile measurements and added to the measured CO_2 flux to obtain the net ecosystem exchange (NEE). Estimates of daytime ecosystem respiration were obtained from the night-NEE relationship, which is explained further in Xu and Baldocchi (2004). The gross primary productivity (GPP) was obtained by taking the difference of NEE and ecosystem respiration. All GPP values in this paper represent a daily average in units of g C/m^2/d.

2.3. Soil moisture sensors

Dynamax Theta probes were installed in the spring of 2001 at depths of 10, 25, 50, and 100 cm as part of three IMZ's in IMS and four in RMS. Soil moisture sensors at 10 and 25 cm were removed from all IMZ's during planting and harvest periods and then reinstalled in the same location.

The soil moisture probes were installed at a 45° angle from vertical to the surface at 10 and 25 cm and were installed using the drip loop method at 50 and 100 cm. Theta probes contain a waterproof enclosure, sensing head, and a cable. The enclosure has a measurement circuitry and an oscillator, while the sensor head consists of three outer rods that surround an inner rod. The rods act as a transmission line and develop an impedance that is dependent on the dielectric constant of the soil. Topp et al. (1980) showed that a linear relationship exists between the volumetric water content and the dielectric constant. Thus, soil volumetric water content (θ) is the standard soil water variable in the CSP, as in the Nebraska AWDN (Hubbard et al., 2009; You et al., 2010).

Soil water data from the CSP underwent significant quality control before its release. Data that were classified as questionable were replaced by previous day's values if only 1 day was bad and by linear interpolation if more than 1 day was bad. Meteorological data from the IMZ's were examined for incidence of precipitation prior to use of interpolation. Automated soil moisture measurements were collected hourly and averaged daily over the span of the project.

2.4. Soil water calculations

Each field only has one eddy covariance tower and thus, only one set of measurements of ET, GPP, and related parameters; the nature of these measurements leads to their representation of a footprint. It is therefore necessary to scale up soil water measurements from point values to aerial values before comparisons can be made with ET. The footprints of the IMZ's are not equal in area and thus field-averaged calculations of soil water are weighted by Equation 1 below, where w_i is the weight (i.e., fraction of the field represented by the fuzzy classes associated with the i'th IMZ), x is the measured soil water in the i'th IMZ and i increases from 1 to n (the total number of IMZs per field). Weights were assigned to each IMZ based on the proportional area of the fuzzy class represented.

$$x = \sum_{i=1}^{n} w_i x_i \quad (1)$$

Prior to the study, soil samples were collected from all IMZ's at the three sites and were analyzed in the laboratory for soil type and water holding capacity. Silt clay loam is the predominant soil texture at IMZ's in both fields. Field capacity and wilting point values at the three sites were determined by averaging the −1/3 bar values and the −15 bar values respectively from moisture release curves determined in the laboratory. A fraction of available soil water (F_{AW}) was calculated via Eq. (2) for a direct comparison of available soil water between IMS and RMS and is used hereafter for soil water comparisons in this paper. The F_{AW} is weighted by IMZ (refer to Eq. (1)) and weighted by root density of maize (Tufekcioglu et al., 1999) to obtain a field average F_{AW}. Values of F_{AW} range from 0 at the wilting point (θ_{WP}) to 1 at field capacity (θ_{FC}), though values over 1 are possible for short periods if θ is between saturation and field capacity.

$$F_{AW} = \frac{(\theta - \theta_{WP})}{\theta_{FC} - \theta_{WP}} \quad (2)$$

2.5. Development stages

The dates of specific development stages of maize were determined from records collected during regular field observations of growth throughout the available years of the CSP. There was usually a slight variation in a development stage within a field, so the date listed for a particular development stage of maize is a date when approximately 50% of the field was at that stage.

2.6. Calculation of SPI and SPEI

Since precipitation is generally not normally distributed, it is necessary to apply a transformation to the probability of observed precipitation for a set time period (i.e., 1-month, 3-months, etc...) to obtain a normalized index. A three-parameter Pearson-Type III distribution was found to be the best universal model for calculation of the SPI (Guttman, 1999), although a two-parameter gamma distribution was also shown to yield good results. The cumulative probability distribution is then transformed into a standard normal distribution using an approximate conversion from Abramowitz and Stegun, 1965. The values for the SPI are analogous to the number of standard deviations above or below the mean and generally range from −3.0 to 3.0. For a more thorough description of the SPI calculation, refer to Lloyd-Hughes and Saunders, 2002.

The SPEI (Vicente-Serrano et al., 2010) is based on the difference (D) between precipitation and ET_p for a period of time, i, as given in Eq. (3):

$$D_i = P - ET_p \quad (3)$$

Table 1
Maize cultivars and planting, harvest, and growth stage dates by season. Yields are adjusted to 15% moisture.

Site/year	Crop/cultivar	Plant pop. (plants/ha)	Planting date	R1 date	PM date	Harvest date	Grain yield (Mg/ha)
IMS							
2003	M/Pioneer 33B51	84,329	14-May	25-July	12-September	14-October	14.0
2005	M/Pioneer 33B51	83,200	2-May	14-July	14-September	18-October	13.2
2007	M/Pioneer 31N28	78,708	1-May	17-July	16-September	6-November	13.2
2009	M/Pioneer 32N72	81,509	21-April	21-July	29-September	10-November	14.2
RMS							
2003	M/Pioneer 33B51	64,292	13-May	23-July	4-September	16-October	7.7
2005	M/Pioneer 33G66	60,117	2-May	18-July	16-September	18-October	9.1
2007	M/Pioneer 33H26X	62,090	1-May	13-July	8-September	1-November	10.2
2009	M/Pioneer 33T57	61,777	22-April	16-July	14-September	11-November	12.0

where P is precipitation (mm) and ET_p is the Thornthwaite method for potential ET. Mavromatis (2007) showed that other methods of ET_p are not necessarily superior when used in calculation of a drought index and the Thornthwaite method requires fewer inputs than other methods, such as Penman–Monteith. Thus, the Thornthwaite method was used for ETp in the calculation of the SPEI in this study.

The process for calculation of the SPEI is slightly more complex than that of the SPI in part because the distribution of D_i is very likely to contain negative values. Thus, a three-parameter distribution is required for the SPEI, whereas a two-parameter gamma distribution can suffice for the SPI. L-moment ratio (Hosking, 1990) diagrams are used for D_i as it allows for the comparison of the empirical frequency of the series with different theoretical distributions. The L-moment ratios are adjusted by a three-parameter log-logistic distribution to obtain a cumulative probability distribution. From there, the calculation of the SPEI follows the steps of the SPI calculation. For further SPEI calculation details, refer to the step-by-step procedure outlined in Vicente-Serrano et al. (2010).

A 1- and 9-month SPI and SPEI are used for comparison in this study. Both indices were calculated at 10-day intervals beginning with 30 May (DOY 150) and ending with 7 September (DOY 250). The Applied Climate Information System (Hubbard et al., 2004) was used to collect data used for analysis in this paper. Data for the SPI and SPEI come from nearby Lincoln, NE. Data used in the study come from multiple locations in Lincoln, though the majority of the period of record comes from the Lincoln Municipal Airport Automated Surface Observing System (ASOS) station (KNLK), which is 40 km to the southwest. Distance between KLNK and the CSP site(s) is sufficient to explain 90% of variation in maximum temperature and just outside the distance to explain 90% of variation in precipitation and minimum temperature (Hubbard, 1994).

There are potential flaws with this method and thus do not expect the indices to match conditions at CSP exactly. However, the long period of record from Lincoln captures severe historical droughts (i.e., 1930s and 1950s), which stations closest to Mead do not. Therefore, the 2003 drought is put in a more representative "historical" context when using data from Lincoln, even if the distance from Lincoln to the CSP sites is too far to match the maximum possible variation in meteorological data. Thus, we believe the sites are close enough such that normalized indices calculated from Lincoln are sufficient for approximating the same indices over the CSP.

3. Results and discussion

3.1. Field management and weather conditions

Table 1 shows details about crop management, cultivars, final grain yield, and dates of planting, harvest, reproductive stage entry, and beginning of physiological maturity at IMS and RMS in years where maize was the common crop. The planting density at RMS under maize was about 75% of IMS, with an average of 62,069 plants/ha over the 4 years compared to an average planting density for 81,937 plants/ha for IMS. In 2003, planting densities were 84,329 and 64,292 plants/ha at IMS and RMS respectively. Maize was planted on 13–14 May at both sites in 2003.

The 2003 growing season began with relatively wet conditions as 146 mm of precipitation fell at RMS in the 30 days prior to planting (Table 2). Precipitation over 1 mm occurred on 16 days between planting and the first week of July, with precipitation over 15 mm occurring four times in that period. However, after receiving 31 mm in a 5 day period from 5 July to 9 July, a long period with minimal or no precipitation was observed at RMS. Between 10 July and 18 August, only 10 mm of precipitation was observed at RMS. Precipitation totaled only 446 mm and 439 at IMS and RMS respectively during the season. The lack of precipitation, particularly during the critical reproductive stage, led to frequent irrigation applications at IMS, with a total of 344 mm applied throughout the season (Table 2). Significant precipitation returned after maize at RMS had reached maturity but minimal precipitation in the critical stages of maize contributed to the significant reductions in yield at RMS.

The long dry spell was also accompanied by 12 days of maximum temperatures (T_{max}) $\geq$35 °C at RMS. Temperatures over 35 °C can be detrimental to maize development and reduce yield (Nield and Newman, 1990), particularly when those temperatures are concurrent with water stress in the first few weeks after silking. Most of the days with $T_{max} \geq 35$ °C occurred during the week of silking onset and again in the period from 16 August to 26 August. The latter period of heat corresponded to the late dough-early dent stage for maize at RMS. The season's highest temperature of 38 °C was reported on both 18 August and 25 August respectively. Vapor pressure deficits (VPD) were also higher during this period and indicative of flash drought conditions, with averages of 1.17 and 1.20 kPa in July and August 2003 compared to the 8-year averages of 0.98 and 0.76 kPa for July and August respectively. Cooler temperatures returned to the area at the end of August in 2003 and the first freeze was reported on 29 September, more than two weeks after maize reached maturity. Thus, final grain yields were not adversely affected by an early freeze in 2003.

A holistic view of the 2003 growing season shows that the four phases described in Illston et al. (2004) accurately describe the May–October 2003 time series of soil moisture data used in this

Table 2
Precipitation (IMS, RMS) and irrigation (IMS) between maize stages.

Time period	RMS precip. (mm)	IMS irrigation (mm)	IMS total (mm)
30 days before planting	146	0	133
Planting to R1	138	108	252
R1 to PM	40	212	269
PM to harvest	115	24	136
Total	439	344	790

Table 3
Average F_{AW}, total precipitation, ET and GPP by phase at IMS and RMS.

Phase	F_{AW}		ET (mm)		GPP (gC/m^2)		Precip. (mm)	
	IMS	RMS	IMS	RMS	IMS	RMS	RMS	IMS
Moist	0.89	0.85	134	128	130	142	197	
Drying	0.67	0.55	197	176	796	721	44	
Stressed	0.7	0.25	200	133	774	543	76	
Recharge	0.76	0.52	79	50	131	36	73	

study. There was a *moist phase* from early May to 25 June, a *drying phase* from 26 June to 1 August, a *stressed phase* from 1 August to 10 September, and a *recharge phase* for the remainder of the season (Fig. 1). The drying (recharge) date was selected as the date when a clear downward (upward) trend in F_{AW} began at RMS and the stressed phase was chosen as the date when the composite F_{AW} at RMS became less than 0.3. The average FAW and the total precipitation, ET, and GPP for each phase are given in Table 3.

Fig. 2 shows that the drying phase at RMS was initially only limited to the top two depths (10 and 25 cm) and closely mirrored the decline in soil water at IMS. Soil water at 50 cm for IMS and RMS initially was somewhat lower than the other depths, due most likely to a lack of full soil recharge in the previous cold season. Nevertheless, the F_{AW} at 50 cm also began to decline by the middle of the drying phase, albeit at a more accelerated rate at RMS than at IMS, where irrigation treatments prevented further decline. By the end of the drying phase, soil water at 100 cm had begun to be depleted at RMS and was significant by the commencement of the stressed phase. Thus, a great divergence in F_{AW} between RMS and IMS at all four depths was evident by the end of the drying phase and this difference in soil water availability led to stark differences in ET and GPP accumulation (Fig. 3) and eventually in grain yield (Suyker and Verma, 2008, 2009, 2012). The difference in ET rates caused by water stress is illustrated further by the ratio of RMS ET to IMS ET in Fig. 4. The ratio started decreasing slightly when F_{AW} at RMS fell to 0.5 and continued to decrease at this rate until F_{AW} was 0.3. The daily rates of ET at RMS relative to the well-watered IMS became very significant once F_{AW} fell below 0.3, which resembles the soil water-ET relationship reported in Waring and Running (1998).

The 1-month standardized drought indices (SPI and SPEI) closely matched conditions on the ground in Mead with the SPI and SPEI going from 1.13 and 1.22 respectively on 29 June to −1.78 and −1.43 respectively on 29 July (Fig. 5). Conversely, the 3- and 9-month indices fell much more slowly during the drying phase and were significantly higher than the 1-month indices by 29 July (Fig. 5). For example, while the 1-month SPI (SPEI) had fallen to −1.78 (−1.43) on 29 July, the 3-month SPI had only dropped to 0.06 (0.19). The 9-month SPI and SPEI were somewhat more indicative of the drying phase by 29 July, but that was as much a result of dry conditions early in the 9-month period than the drought that had developed in the preceding weeks.

The 1-month SPI and the 1-month SPEI increased during the stressed phase and were at −0.9 by 18 August as a result of precipitation, which also corresponded with a brief increase in the F_{AW} at RMS (refer to Figs. 1 and 2). However, the magnitude of the increase in the 1-month indices was partly a result of an additional 20 mm of precipitation falling at nearby Lincoln, NE than at RMS in the period from 31 July to 4 August. Therefore, it is likely that the 1-month SPI and SPEI were somewhat underestimating the severity of the dryness during the stressed phase at RMS, which in turn demonstrates the main disadvantage of using a nearby weather station as a proxy for meteorological data when calculating a drought index.

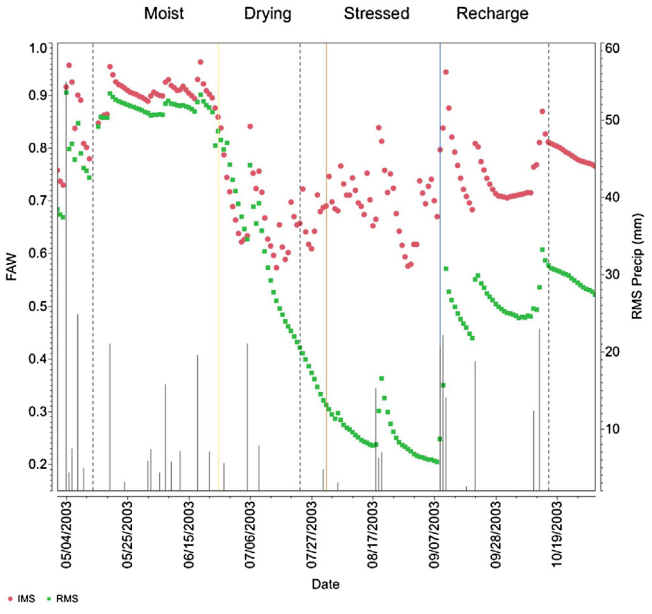

Fig. 1. Daily average F_{AW} at IMS (red circles) and RMS (green squares) and total daily precipitation at RMS (black needles). Dashed vertical lines indicate the planting, silking, and harvest dates at RMS respectively. The inception of the drying, stressed, and recharge phases are indicated by the yellow, orange, and blue vertical lines respectively. (For interpretation of the references to color in this figure legend, the reader is referred to the web version of the article.)

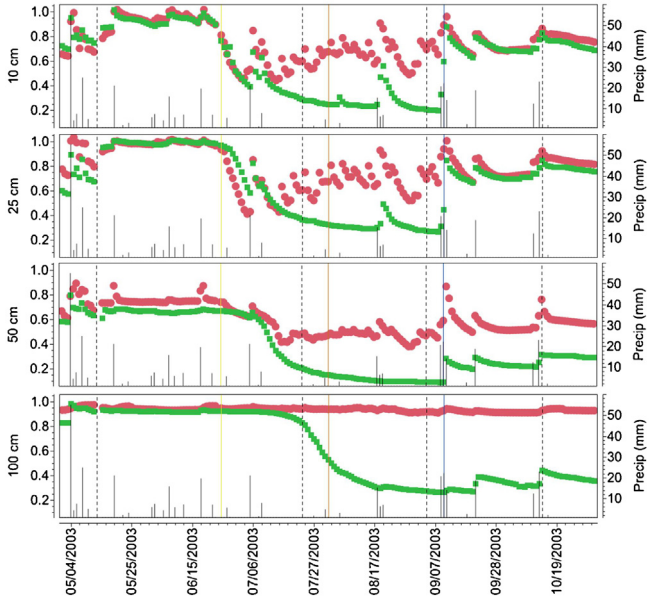

Fig. 2. From top to bottom, daily average F_{AW} at IMS (red) and RMS (green) at 10, 25, 50, and 100 cm respectively. Total daily precipitation at RMS is indicated black needles. Dashed vertical lines indicate the planting, silking, and harvest dates at RMS respectively. The inception of the drying, stressed, and recharge phases are indicated by the yellow, orange, and blue vertical lines respectively. (For interpretation of the references to color in this figure legend, the reader is referred to the web version of the article.)

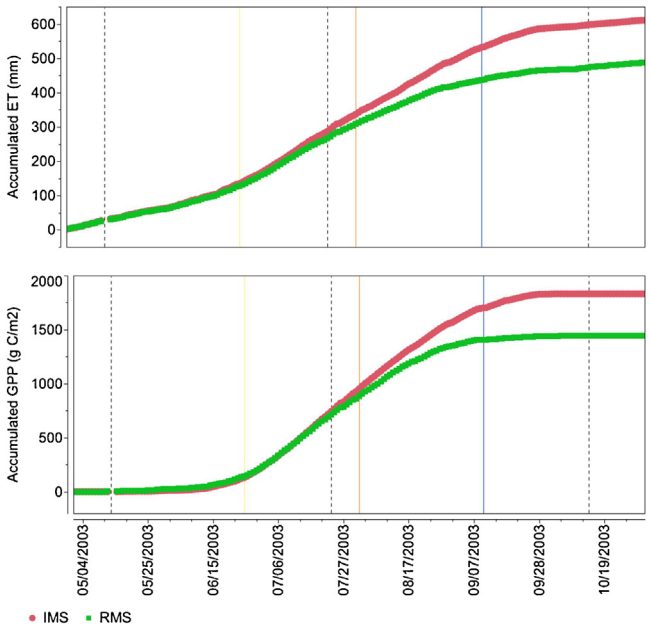

Fig. 3. Accumulated evapotranspiration (top) and gross primary productivity at IMS (red) and RMS (green). Dashed vertical lines indicate the planting, silking, and harvest dates at RMS respectively. The inception of the drying, stressed, and recharge phases are indicated by the yellow, orange, and blue vertical lines respectively. (For interpretation of the references to color in this figure legend, the reader is referred to the web version of the article.)

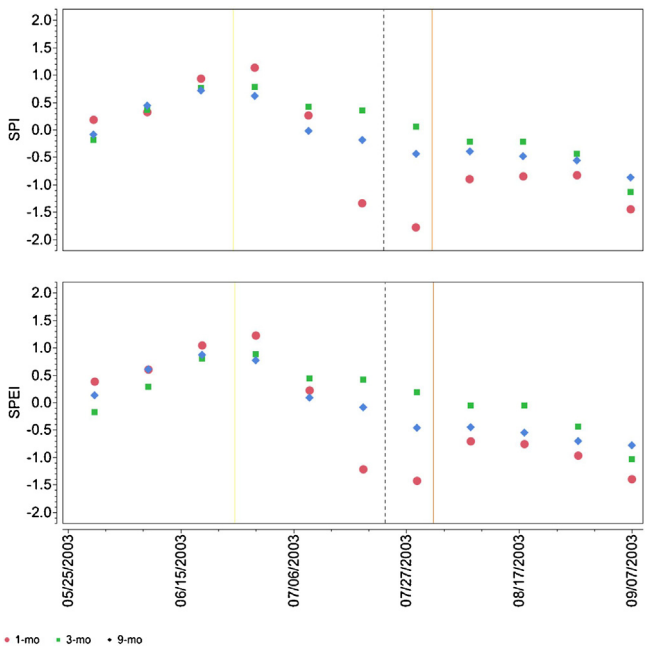

Fig. 5. 1-, 3-, and 9-month SPI (SPEI) on top (bottom). The dashed vertical line indicates the silking date and the yellow and orange lines indicate the inception of the drying and stressed phases respectively. (For interpretation of the references to color in this figure legend, the reader is referred to the web version of the article.)

The remainder of this section of the paper is setup to look at the relationship of these parameters (i.e., soil water, ET, GPP) during individual phases in more detail. Since the first three phases coincided with maize being in the vegetative and/or reproductive stages, soil water (both composite and by individual depth), ET accumulation, and GPP accumulation at RMS are compared with IMS. The recharge phase occurred after maize at RMS had reached maturity and thus only soil water comparisons are applicable. The 1- and 9-month drought indices (i.e., SPI and SPEI) are also discussed during the subsections for the individual phases (except the recharge phase).

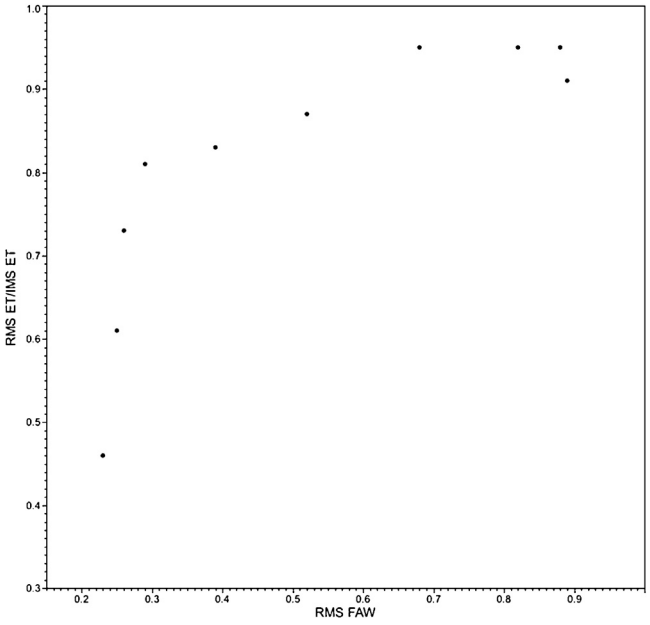

Fig. 4. Ratio of total evapotranspiration at IMS to RMS versus the F_{AW} at RMS over 10-day periods during the growing season.

3.2. Moist phase

Significant precipitation fell over the region about 10 days before planting, which led to an increase in F_{AW} at both sites and elimination of the difference in F_{AW} between the two sites at 100 cm (Fig. 6). Adequate precipitation during the rest of the moist phase allowed for a nearly identical F_{AW} at 10, 25, and 100 cm and only slightly higher F_{AW} at IMS than RMS at 50 cm. Equivalent amounts of soil water between the two sites led to nearly identical daily rates of ET, with IMS pulling slightly ahead in accumulated ET by the end of the moist phase (Fig. 7). That is to be expected however, as a higher population density of maize at IMS would lead to a bit more ET than at RMS, all other things being "equal".

Fig. 7 also shows that GPP accumulation started about 10 days after planting and accumulation rates were almost identical between the two sites during the moist phase. Fig. 8 further demonstrates that the average hourly rates of GPP during a 10-day period (DOY 171–180) during the moist phase were nearly identical throughout the day. The maize crop was entering the V6 (six-leaf) stage at the beginning of the aforementioned 10-day period so rates of GPP accumulation were lower than later in the season, particularly at IMS. The 1- and 9-month SPI and SPEI had similar values throughout the moist phase and were responsive to the moist and relatively cool conditions. The 1-month (9-month) SPI and SPEI were at 1.13 and 1.22 (0.62 and 0.77) respectively by late June.

3.3. Drying phase

A period of dry weather in late June lowered the F_{AW} at both sites to around 0.60 and thus commenced the drying phase. The F_{AW} returned to 0.86 and 0.80 at IMS and RMS respectively after 21 mm of precipitation on 5 July, but the recharge was very short-lived. The extended period of dry weather combined with a high crop water demand quickly depleted the soil water at RMS and caused

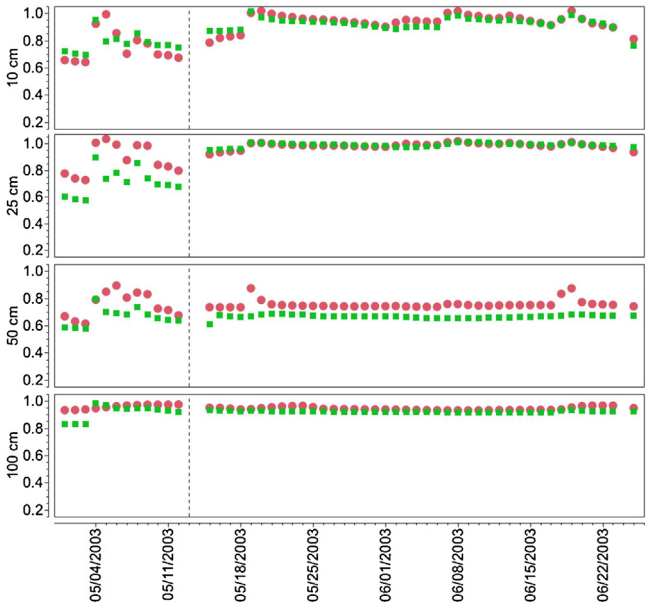

Fig. 6. From top to bottom, comparison of fraction of available water (FAW) at 10, 25, 50, and 100 cm respectively at IMS (red circles) and RMS (green squares) during the moist phase. Dashed vertical line indicates planting date of maize at RMS. (For interpretation of the references to color in this figure legend, the reader is referred to the web version of the article.)

irrigation treatments to be applied at IMS every 5–6 days for the rest of the drying phase. The F_{AW} at 25 cm at IMS was initially lower than at RMS, which could be attributed to a higher plant population density leading to greater soil water demand at IMS than at RMS.

Fig. 9 shows that the irrigation treatments at IMS led to the (approximate) 5-day moistening-drying cycle at 10 and 25 cm and the prevention of large soil water depletion at the deeper depths,

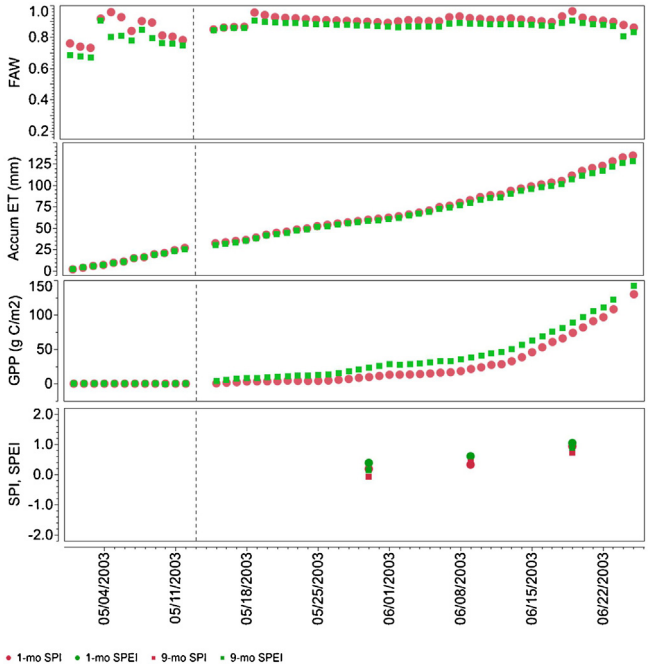

Fig. 7. From top to bottom, a comparison of Fraction of Available Water (FAW), accumulated evapotranspiration (ET), accumulated gross primary productivity (GPP) for IMS (red circles) and RMS (green squares), and a 1- and 9-month SPI and SPEI during the moist phase of the 2003 growing season. Dashed vertical line indicates planting date of maize at RMS. (For interpretation of the references to color in this figure legend, the reader is referred to the web version of the article.)

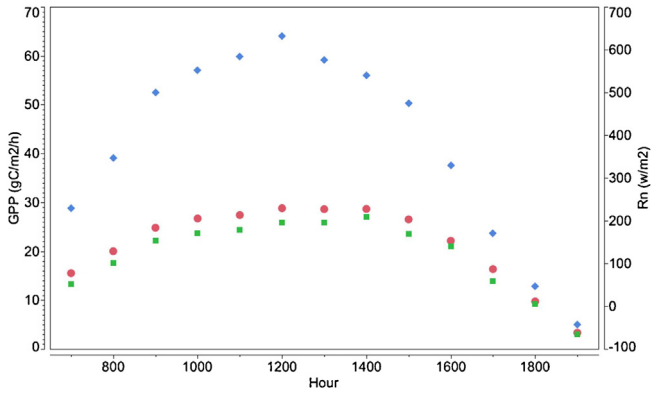

Fig. 8. Average hourly GPP (left *y*-axis) at IMS (red circles) and RMS (green squares) compared to the median hourly net radiation over a 10-day period (DOY 171–180) during the moist phase. Time shown on the *x*-axis is central standard time (CST). (For interpretation of the references to color in this figure legend, the reader is referred to the web version of the article.)

particularly after mid-July. By the end of the drying phase, F_{AW} at RMS was 0.42, 0.35, 0.31, and 0.38 less than the corresponding F_{AW} at 10, 25, 50, and 100 cm respectively.

The reduction in soil water led to lower daily rates of ET and accumulated GPP at RMS compared to IMS (Fig. 10). The reduction in ET at RMS was less significant at first and the difference between RMS and IMS was less than 1.0 mm/day, such that the difference in accumulated ET between IMS and RMS increased from 6 to 27 mm between the beginning and end of the drying phase. GPP accumulation was also affected by the decline in soil water at RMS, going from 10 $gC/m^2/h$ greater than IMS at the beginning of the drying phase to 63 $gC/m^2/h$ less than IMS by the end of the drying phase.

Plants under water stress close stomata as a direct signal from the metabolic activity of roots under water stress (Schulze, 1986). Thus, the reduction in ET and GPP at RMS implies stomatal conductance of maize at RMS was reduced compared to that of maize at IMS. Fig. 11 adds validation to this by showing the

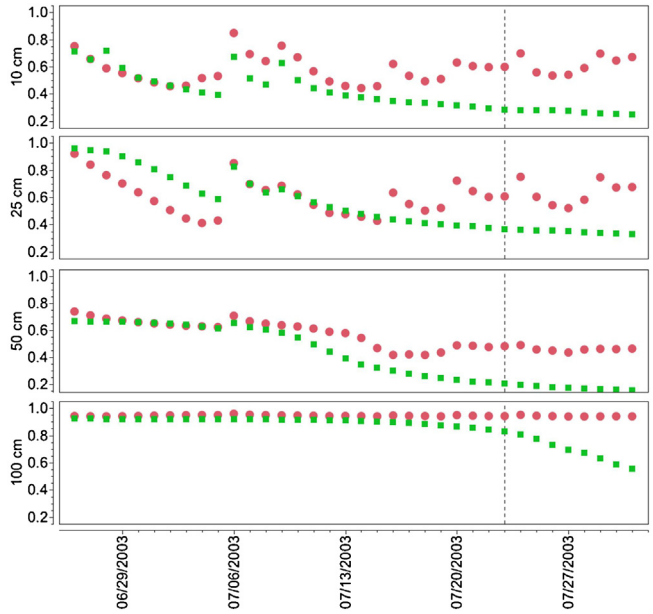

Fig. 9. From top to bottom, comparison of fraction of available water (FAW) at 10, 25, 50, and 100 cm respectively at IMS (red circles) and RMS (green squares) during the drying phase. Dashed vertical line indicates silking date of maize at RMS. (For interpretation of the references to color in this figure legend, the reader is referred to the web version of the article.)

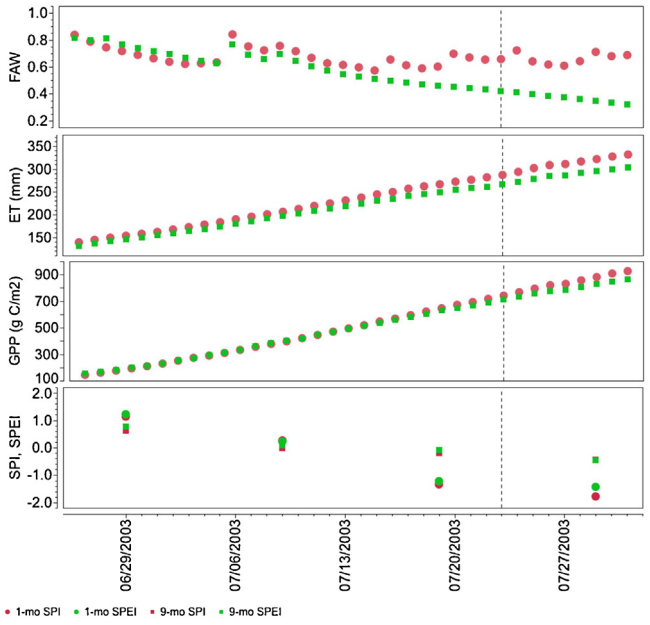

Fig. 10. From top to bottom, a comparison of Fraction of Available Water (FAW), accumulated evapotranspiration (ET), accumulated gross primary productivity (GPP) at IMS (red circles) and RMS (green squares), and a 1- and 9-month SPI and SPEI during the drying phase of the 2003 growing season. Dashed vertical line indicates silking date of maize at RMS. (For interpretation of the references to color in this figure legend, the reader is referred to the web version of the article.)

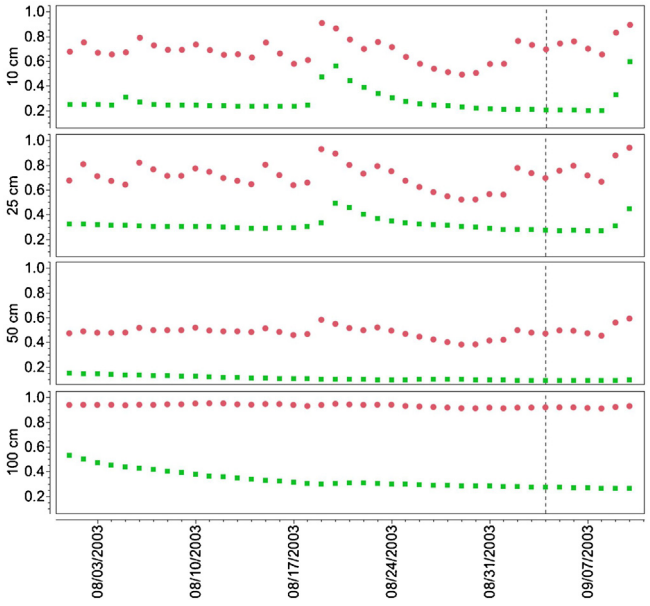

Fig. 12. From top to bottom, comparison of fraction of available water (FAW) at 10, 25, 50, and 100 cm respectively at IMS (red circles) and RMS (green squares) during the stressed phase. Dashed vertical line indicates maturity date of maize at RMS. (For interpretation of the references to color in this figure legend, the reader is referred to the web version of the article.)

divergence in average hourly GPP at RMS compared to that of IMS during peak hours of peak net radiation over a 10-day period (DOY 201–210) in the drying phase. For example, during the hour ending at 1100 LST, the average GPP accumulations at IMS and RMS were 67 and 51 gC/m^2/h respectively. Maize was entering the reproductive stage at both sites during this period and thus, hourly GPP accumulation was much more significant than during the 10-day period in the moist phase.

Both the 1-month SPI and SPEI were extremely responsive to the dry spell, dropping from 1.13 and 1.22 respectively to −1.78 and −1.43 respectively during the five weeks of the drying phase. The 9-month SPI and SPEI slowly declined from 0.62 and 0.77 to −0.44 and −0.46 respectively. Thus, the shorter-term drought indices proved to be quite responsive to the onset of the dry spell during the drying phase. It was originally thought that the SPEI would be more negative but a closer look at temperatures during the drying phase showed that there were enough cooler days mixed in with days of maximum temperatures over 35 °C to keep temperatures close to the long-term average of around 25 °C during the period.

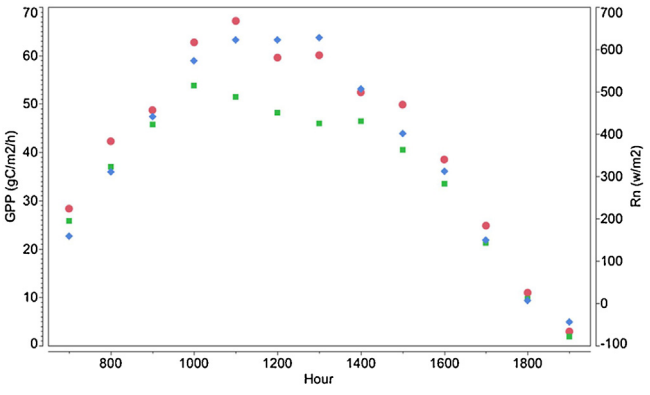

Fig. 11. Average hourly GPP (left *y*-axis) at IMS (red circles) and RMS (green squares) compared to the median hourly net radiation over a 10-day period (DOY 201–210) during the drying phase. Time shown on the *x*-axis is central standard time (CST). (For interpretation of the references to color in this figure legend, the reader is referred to the web version of the article.)

3.4. Stressed phase

The stressed phase began on 1 August when F_{AW} at RMS dropped below 0.30. Fig. 12 shows that with the exception of a temporary increase (and quick subsequent decrease) in F_{AW} at 10 and 25 cm following precipitation on 18–20 August, F_{AW} at 10, 25, and 50 cm declined very slowly or held steady during the stressed phase. This implies that nearly all soil water taken up by maize at RMS was coming from below 50 cm. Indeed, the RMS F_{AW} at 100 cm continued to decline steadily during the first few weeks of August before leveling out at approximately 0.27 for the remainder of the stressed phase. Frequent irrigation treatments at IMS kept FAW above 0.6 at 10 and 25 cm, around 0.5 at 50 cm, and close field capacity at 100 cm during this phase. Thus, water stress was not a factor at IMS and the stressed phase ended on 10 September when significant precipitation increased the F_{AW} at RMS to over 0.30.

As referenced in the discussion of the drying phase, stomatal conductance is reduced during periods of water stress, and this was clear during the stressed phase at RMS. Daily ET rates widened further in the stressed phase as IMS averaged 4.8 mm/day and RMS averaged 3.1 mm/day, such that a difference of 94 mm existed by the end of the stressed phase (Fig. 13). GPP was also greatly affected and the difference in accumulated GPP increased to 294 gC/m^2 between IMS and RMS during the stressed phase. Perhaps the most striking evidence of reduced stomatal conductance comes from Fig. 14. At well-watered IMS, the average hourly accumulation over a 10-day period (DOY 221–230) closely follows the net radiation curve and peaks at 1100 CST at 62 gC/m^2, indicating that little to no stress was put on the crop (i.e., little to no inhibition on photosynthesis). Meanwhile at the water-stressed RMS, hourly GPP accumulation began to level out early in the morning and peaked at 46 gC/m^2 at 1100 CST, adding more evidence of water stress significantly reducing stomatal conductance.

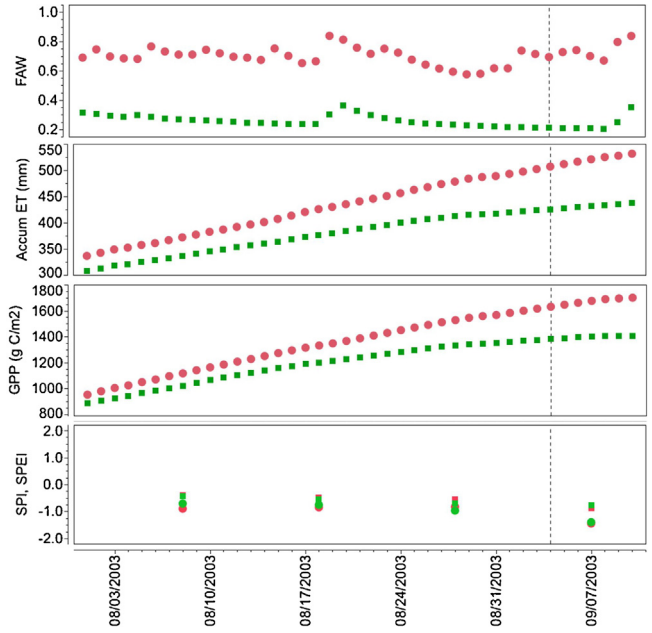

Fig. 13. From top to bottom, a comparison of Fraction of Available Water (FAW), accumulated evapotranspiration (ET), accumulated gross primary productivity (GPP) for IMS (red circles) and RMS (green squares), and a 1- and 9-month SPI and SPEI during the stressed phase of the 2003 growing season. Dashed vertical line indicates maturity date of maize at RMS. (For interpretation of the references to color in this figure legend, the reader is referred to the web version of the article.)

The 1-month SPI and SPEI did not match conditions on the ground as well in the stressed phase as they did in the drying phase. This was due mostly to an additional 18 mm that fell at the Lincoln site compared to Mead on 31 July that temporarily brought the 1-month indices above −1.0. The brief rise was short-lived though and both of the 1-month indices captured the subsequent decline in soil water at RMS during a period of twenty consecutive days without precipitation that began on 21 August. The 1-month SPI and 1-month SPEI declined below −1.4 shortly after the onset of physiological maturity (4 September; DOY 247) and the 9-month SPI and SPEI declined steadily over the last month of the stressed phase to −0.87 and −0.78 respectively. Therefore, the 9-month SPI and SPEI were somewhat more indicative of the flash drought by the end of the stressed phase than they had been at the end of the drying phase.

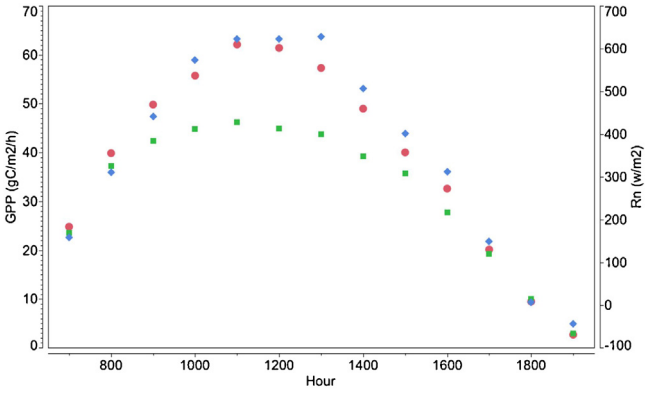

Fig. 14. Average hourly GPP (left *y*-axis) at IMS (red circles) and RMS (green squares) compared to the median hourly net radiation over a 10-day period (DOY 221–230) during the stressed phase. Time shown on the *x*-axis is central standard time (CST). (For interpretation of the references to color in this figure legend, the reader is referred to the web version of the article.)

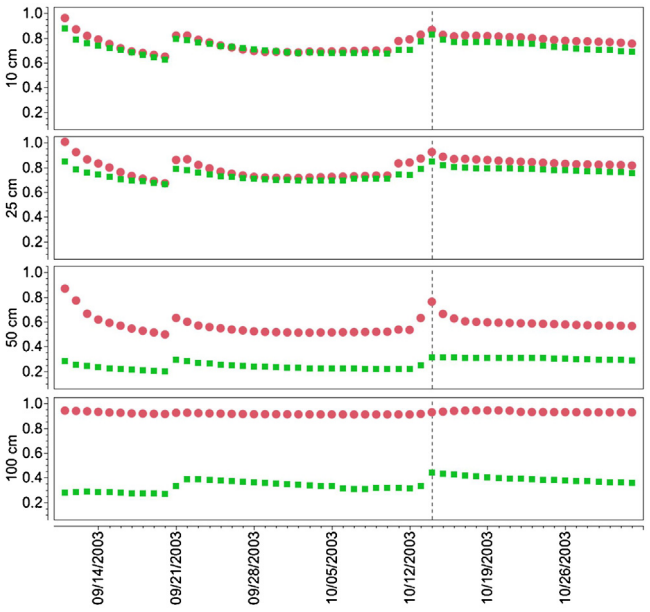

Fig. 15. From top to bottom, comparison of fraction of available water (FAW) at 10, 25, 50, and 100 cm respectively at IMS (red circles) and RMS (green squares) during the recharge phase. Dashed vertical line indicates date of maize harvest at RMS. (For interpretation of the references to color in this figure legend, the reader is referred to the web version of the article.)

3.5. Recharge phase

Significant precipitation did return to Mead as 56 mm fell over a 3-day period from 9 to 11 September. It was too late to rejuvenate the maize at RMS unfortunately as physiological maturity had been achieved days earlier. However, Fig. 15 shows that the precipitation from 9 to 11 September brought the 10 cm F_{AW} at IMS to near field capacity and the F_{AW} at RMS to 0.87. Significant recharge also occurred at 25 cm as field capacity was realized at IMS and the F_{AW} at RMS increased to 0.85. Some recharge also occurred at 50 cm, though there was still a very large difference in F_{AW} between IMS and RMS.

The remainder of the recharge phase was not exceptionally wet, as only 59 mm fell between 11 September and 1 November. But, the combination of maturing crops and cooler temperatures led to a low demand for soil water (i.e., precipitation at RMS was greater than ET) and this was sufficient to keep 10 and 25 cm moist at both sites. It also permitted some additional recharge at 50 cm at both IMS and RMS and at 100 cm at RMS. Perhaps the most interesting aspect of Fig. 15 is how the time series of F_{AW} at 10 cm and 25 cm in the recharge phase resembles that of the moist phase, as the difference in F_{AW} was minimal between IMS and RMS. Conversely, the time series of F_{AW} at 50 and 100 cm more closely resembles that of the stressed phase, as large differences in F_{AW} between IMS and RMS remained, even with some recharge at RMS. Thus, true recharge only occurred at 10 and 25 cm at Mead in 2003, even though there was improvement at the deeper depths.

4. Conclusions

The grain yield of 7.7 Mg/ha at RMS in 2003 was only a little more than half of the grain yield at IMS (14.0 Mg/ha). For the sake of comparison, during the more optimal 2009 growing season, RMS had a final grain yield of 12.0 Mg/ha (Table 1). While it is doubtful that the final yield at RMS would have equaled the yield of IMS had the 2003 season remained moist, the yield in 2009 gives a useful comparison for how much yield was potentially lost to the flash drought in 2003. The term flash drought is appropriate for this case study for

two key reasons. The first reason is precipitation was adequate and soils were moist for the first 2 months post-maize planting, which led to comparable rates of ET and GPP accumulation between IMS and RMS during the moist phase of the season. Thus, the initiation of drought was well-defined by actual measurements of precipitation and other agro-meteorological variables.

The second reason is that a prolonged stretch with minimal precipitation occurred during the most critical growth stages for maize and coincided with the drying and stressed phases discussed earlier. It can be implied that the lack of precipitation and decline in soil water at RMS led to corresponding decreases in stomatal conductance, which in turn led to reductions in photosynthesis as evidenced by the significant differences in GPP accumulation, total ET, and final grain yield between RMS and IMS. In contrast, when precipitation was adequate and soil water differences between the two sites were negligible in the moist phase, both sites had nearly identical levels of accumulated ET.

The difference in accumulated ET and GPP between IMS and RMS widened considerably after early August, which closely coincides with the period where soil water at 100 cm went from a linear decrease to a more curvilinear decrease. The timing of the water stress was critical at RMS as the low decline in the ET rate that occurred as maize began silking (23 July; DOY 204) accelerated as maize went through the critical reproductive stage. The irrigated maize at IMS had no discernible water stress and ET rates remained steady throughout the reproductive stage. Significant impacts were therefore realized because of the timing of the drought at RMS. Thus, it can be stated that a flash drought can by characterized by, but not limited to, a well-defined inception with severe impacts on vegetation, including grain crops such as maize, and can be of relatively short duration if a recovery period occurs within a few months of the drought's inception.

This study also confirmed the effectiveness of using a 1-month SPEI and a 1-month SPI for purposes of flash drought detection. Results showed that both 1-month indices were robust at detecting the onset of the flash drought (i.e., in the drying phase) when compared with the 9-month indices as they matched the decline of soil water at RMS very well. The two indices were close throughout the season, indicating that temperatures were close to historical averages over the course of the growing season. While there were indeed several days of temperatures over 35 °C in the 2003 growing season, the 2003 season overall was not an excessively hot summer by standards of the western U.S. Corn Belt, and thus the SPEI was not necessarily a better indicator of the flash drought in this study. However, the SPEI yields vital information about the effect of temperature in a drought, and it is likely that the SPEI will be a more robust indicator of drought than the SPI in some future studies. Future work will also be needed to determine if the relationship between indices calculated over different time scales (i.e., 1-month, 9-months, etc.. . .) are similar to what was reported in this study.

Acknowledgments

The research presented here was supported by the Office of Science (BER), U.S. Department of Energy Grant (No. DE-FG02-03ER63639 and the University of Nebraska-Lincoln Program of Excellence. Special thanks to Todd Schimelfenig, Dave Scoby, and Glen Roebke for providing technical expertise and data.

References

Abramowitz, M., Stegun, I., 1965. Handbook of Mathematical Functions. Dover Publications, New York.

Baldocchi, D.D., 2003. Assessing the eddy covariance technique for evaluating carbon dioxide exchange rates of ecosystems: past, present, and future. Global Change Biol. 9 (4), 479–492.

Baldocchi, D.D., Hicks, B.B., Meyers, T.P., 1988. Measuring biosphere–atmosphere exchanges of biologically related gases with micrometeorological methods. Ecology 69 (5), 1331–1340.

Basara, J.B., Arndt, D.S., Johnson, H.L., Brotzge, J.G., Crawford, K.C., 1998. An analysis of the drought of 1998 using the Oklahoma Mesonet. EOS Trans. AGU 79, 258.

Brown, J.F., Wardlow, B.D., Tadesse, T., Hayes, M.J., Reed, B.C., 2008. The Vegetartion Drought Response Index (VegDRI): a new integrated approach for monitoring drought stress in vegetation. GISci. Remote Sens. 45, 16–46.

Cakir, R., 2004. Effect of water stress at different development stages on vegetative and reproductive growth of corn. Field Crops Res. 89, 1–16.

Calvino, P.A., Andrade, F.H., Sadras, V.O., 2003. Maize yield as affected by water availability, soil depth, and crop management. Agron. J. 95, 275–281.

Dale, R.F., Shaw, R.H., 1965. Effect on corn yields of moisture stress and stand at two different fertility levels. Agron. J. 57, 475–479.

Denmead, O.T., Shaw, R.H., 1960. The effects of soil moisture stress at different stages of growth on the development and yield of corn. Agron. J. 52, 272–274.

Earl, H.J., Davis, R.F., 2003. Effect of drought stress on leaf and whole canopy maize radiation use efficiency and yield of maize. Agron. J. 95, 688–696.

Guttman, N.B., 1999. Accepting the standardized precipitation index: a calculation algorithm. J. Am. Water Resour. Assoc. 35, 311–322.

Hayes, M., Wilhite, D.A., Svoboda, M., Vanyarkho, O., 1999. Monitoring the 1996 drought using the standardized precipitation index. Bull. Am. Meteorol. Soc. 80, 429–438.

Hayes, M., Svoboda, M., Wall, N., Widhalm, M., 2011. The Lincoln declaration on drought indices: universal meteorological drought index recommended. Bull. Am. Meteorol. Soc. 92, 485–488.

Heim, R.R., 2002. A review of twentieth-century drought indices used in the United States. Bull. Am. Meteorol. Soc. 83, 1149–1165.

Hollinger, S.E., Isard, S.A., 1994. A soil moisture climatology of Illinois. J. Climate 7, 822–833.

Hosking, J.R.M., 1990. L-Moments: analysis and estimation distributions using linear combinations of order statistics. J. R. Stat. Soc. 52 (1), 105–124.

Hu, Q., Willson, G.D., 2000. Effect of temperature anomalies on the Palmer drought severity index in the central United States. Int. J. Climatol. 20, 1899–1911.

Hubbard, K.G., 1994. Spatial variability of weather variables in the high plains of the USA. Agric. For. Meteorol. 68, 29–41.

Hubbard, K.G., DeGaetano, A.T., Robbins, K.D., 2004. A modern applied climate information system. Bull. Am. Meteorol. Soc. 85 (6), 811–812.

Hubbard, K.G., You, J., Sridhar, V., Hunt, E., Korner, S., Roebke, G., 2009. Near-surface soil water monitoring for water resources management on a wide-area basis in the Great Plains. Great Plains Res. 19, 45–54.

Illston, B.G., Basara, J.B., 2003. Analysis of short-term droughts in Oklahoma. EOS Trans. AGU 84 (17), 157.

Illston, B.G., Basara, J.B., Crawford, K.C., 2004. Seasonal to interannual variations of soil moisture measured in Oklahoma. Int. J. Climatol. 24, 1883–1896.

Illston, B.G., Basara, J.B., Fischer, D.K., Elliott, R.L., Fiebrich, C., Crawford, K.S., Humes, K., Hunt, E., 2008. Mesoscale monitoring of soil moisture across a statewide network. J. Atmos. Oceanic Technol. 25, 167–182.

Livida, I., Assemakopoulos, V.D., 2007. Spatial and temporal analysis of drought in Greece using the Standardized Precipitation Index (SPI). Theor. Appl. Climatol. 89, 143–153.

Lloyd-Hughes, B., Saunders, M.A., 2002. A drought climatology for Europe. Int. J. Climatol. 22, 1571–1592.

Mavromatis, T., 2007. Drought index evaluation for assessing future wheat production in Greece. Int. J. Climatol. 27 (7), 911–924.

McKee, T.B., Doesken, N.J., Kleist, J.,1993. The relationship of drought frequency and duration to time scales. In: Preprints, Eighth Conference on Applied Climatology. Am. Meteorol. Soc., Anaheim, CA, pp. 179–184.

McRoberts, B., Nielsen-Gammon, J., 2012. The use of a high-resolution standardized precipitation index for drought monitoring and assessment. J. Appl. Meteorol. Climatol. 51 (1), 68–83.

Meyer, S.J., Hubbard, K.G., Wilhite, D.A., 1993. A crop-specific drought index for corn: I. Model development and validation. Agron. J. 85, 388–395.

Monteith, J.L.,1964. Evaporation and environment. In: The State and Movement of Water in Living Organisms, 19th Symposium, Society for Experimental Biology. Academic Press, New York, pp. 205–234.

Nield, R.E., Newman, N.E., 1990. Growing season characteristics and requirements in the Corn Belt. In: National Corn Handbook. Purdue University, Cooperation Extension Service, West Lafayette, IN.

Palmer, W.C., 1965. Meteorological droughts. U.S. Department of Commerce, Weather Bureau Research Paper 45, 58 pp.

Peterson, T.C., Easterling, W.D.R., Karl, T.A., Groisman, P., Nicholls, N., Plummer, N., Torok, S., Auer, I., Boehm, R., Gullett, D., Vincent, L., Heino, R., Tuomenvirta, H., Mestre, O., Szentimrey, T., Salinger, J., Forland Hanssen-Bauer, I., Alexandersson, H., Jones, P., Parker, D., 1998. Homogeneity adjustments of in situ atmospheric climate data: a review. Int. J. Climatol. 18, 1493–1517.

Schulze, E.D., 1986. Carbon dioxide and water vapor exchange on response to drought in the atmosphere and in the soil. Ann. Rev. Plant Physiol. 37, 247–274.

Suyker, A.E., Verma, S.B., 2008. Interannual water vapor and energy exchange in an irrigated maize-based agroecosystem. Agric. For. Meteorol. 148, 417–427.

Suyker, A.E., Verma, S.B., 2009. Evapotranspiration of irrigated and rainfed maize-soybean cropping systems. Agric. For. Meteorol. 149, 443–452.

Suyker, A.E., Verma, S.B., 2012. Gross primary production and ecosystem respiration of irrigated and rainfed maize-soybean cropping system over 8 years. Agric. For. Meteorol. 165, 12–24.

Suyker, A.E., Verma, S.B., Burba, C.G., 2003. Interannual variability in net CO_2 exchange of a native tallgrass prairie. Global Change Biol. 9, 1–11.
Svoboda, M., Lecomte, D., Hayes, M., Heim, R., Gleason, K., Angel, J., Rippey, B., Tinker, R., Palecki, M., Stooksbury, D., Miskus, D., Stephens, S., 2002. The drought monitor. Bull. Am. Meteorol. Soc. 83 (8), 1181–1190.
Thornthwaite, C.W., 1948. An approach toward a rational classification of climate. Geogr. Rev. 38, 55–94.
Topp, G.C., Davis, J.L., Annan, A.P., 1980. Electromagnetic determination of soil water content: measurement in coaxial transmission lines. Water Resour. Res. 16, 574–582.
Tufekcioglu, A., Raich, J.W., Isenhart, T.M., Schultz, R.C., 1999. Fine root dynamics, coarse root biomass, root distribution, and soil respiration in a multispecies riparian buffer in Central Iowa, USA. Agrofor. Sys. 44, 163–174.
Verma, S.B., Dobermann, A., Cassman, K.G., Walters, D.T., Knops, J.M., Arkebauer, T.J., Suyker, A.E., Burba, G.G., Amos, B., Yang, H., Ginting, D., Hubbard, K.G., Gitelson, A.A., Walter-Shea, E., 2005. Annual carbon dioxide exchange in irrigated and rainfed maize-based agroecosystems. Agric. For. Meteorol. 131, 77–96.
Vicente-Serrano, S.M., Begueria, S., Lopez-Moreno, J.I., 2010. A multiscalar drought index sensitive to global warming: the standardized precipitation evapotranspiration index. J. Climate 23, 1696–1718.
Waring, R.H., Running, S.W., 1998. Forest Ecosystems Analysis at Multiple Scales. Academic Press, New York.
Wilhite, D.A., Glantz, M.H., 1985. Understanding the drought phenomenon: the role of definitions. Water Int. 10, 111–120.
Wu, H., Hayes, M.J., Wilhite, D.A., Svoboda, M.D., 2005. The effect of length of record on the standardized precipitation index calculation. Int. J. Climatol. 25 (4), 505–520.
Xu, L., Baldocchi, D.D., 2004. Seasonal variation in carbon dioxide exchange over a Mediterranean annual grassland in California. Agric. For. Meteorol. 113 (1–4), 223–243.
You, J., Hubbard, K.G., Mahmood, R., Srihar, V., Todey, D., 2010. Quality control of soil water data in applied climate information system – case study in Nebraska. J. Hydrol. Eng. 15, 200–209.